3D-printed EVA-based patches manufactured by direct powder extrusion for personalized transdermal therapies

Giorgia Maurizii[1], Sofia Moroni[1], Shiva Khorshid[1], Annalisa Aluigi[1], Mattia Tiboni[1]*, and Luca Casettari[1,2]

[1]*Department of Biomolecular Sciences, University of Urbino Carlo Bo, Piazza del Rinascimento, 6, 61029 Urbino (PU), Italy.*

[2]*Prosopika srl, Via del Trabocchetto, 1, 61034, Fossombrone (PU), Italy.*

Abstract

In recent years, 3D printing has attracted great interest in the pharmaceutical field as a promising tool for the on-demand manufacturing of patient-centered pharmaceutical forms. Among the existing 3D printing techniques, direct powder extrusion (DPE) has been demonstrated as the most practical approach thanks to its high flexibility, low cost, and simplicity. The main goal of this work was to determine whether different grades of ethylene vinyl acetate (EVA) copolymer might be employed as new feedstock materials for the DPE technique to manufacture transdermal patches. By selecting two model drugs with different thermal behavior, we also wanted to pay attention to the versatility of EVA excipient in preparing patches for customized transdermal therapies. EVA polymeric matrices were loaded with 30% (w/w) of the model drug. Both formulations were successfully processed with the DPE technique. The physicochemical composition of the printed devices was investigated through Fourier-transform infrared spectroscopy, differential scanning calorimetry, and thermogravimetric analyses. Lastly, the drug release and permeation profile of the printed systems was evaluated for 48 hours and showed to be dependent on the VA content of the EVA grade. Hence, this study demonstrated that EVA and direct powder extrusion technique could be promising tools for manufacturing transdermal patches. By selecting the EVA grade with the appropriate VA content, drugs with dissimilar melting points could be printed preserving their thermal stability. Moreover, the desired drug release and permeation profile of the drug can be achieved, representing an important advantage in terms of personalized medicine.

Keywords: Direct Powder Extrusion (DPE); Ethyl vinyl acetate (EVA) copolymer; Transdermal patches; Personalized medicine; Additive manufacturing

1. Introduction

Over the years, in the pharmaceutical field, the concept of a ‘’one-size-fits-all drug’’ has been revised to make room for personalized medicine, thanks primarily to the spreading of three-dimensional printing (3DP) (Vaz et al., 2021). This technology allows the manufacturing of pharmaceutical forms with customized shapes, dosages, release characteristics, and drug combinations. The desired object is produced in a layer-by-layer manner by translating a computer-aided design (CAD) model into a solid prototype (Seoane-Viaño et al., 2021) (Reddy et al., 2020). Between the advantages conferred, in addition to increasing patient compliance and adherence to treatment, this approach reduces fabrication costs and enables the on-site production of medicines, potentially performed in hospitals and pharmacies (Fanous et al, 2020).

Among the existing 3D printing techniques, extrusion-based 3D printing methods, such as Fused Deposition Modeling (FDM) and Direct Powder Extrusion (DPE), are the most used for the on-demand manufacturing of pharmaceuticals, thanks to the low cost, flexibility, and the wide availability of materials and printers (Annaji et al., 2020). FDM is based on the extrusion of a drug-loaded thermoplastic filament, conventionally produced by Hot Melt Extrusion (HME). Despite the successful employment of this technique, the two-step thermal processing can cause material degradation, and the need for a filament with optimal rheological and mechanical properties can limit its use (Xu et al., 2020) (Goyanes et al., 2019). DPE is an alternative to FDM as it permits the direct printing of powder blends and pellets by extrusion through a nozzle, using a single-screw extruder mounted in the printer. By avoiding filament preparation with HME, this single-step production process reduces the thermal stress of active compounds and is more cost-and-time-effective and practical in terms of on-site manufacturing. Moreover, it potentially allows freedom in formulation selection since the material flow toward the printer nozzle is mostly driven by the screw rotation, and it is slightly influenced by the material’s mechanical properties (Borandeh et al., 2021) (Sánchez-Guirales et al, 2021) (Pistone et al., 2022).

Ethylene-vinyl acetate (EVA) is a thermoplastic copolymer of ethylene and vinyl acetate (VA), where the VA units, ranging from 0 % to 40 %, are distributed across the ethylene polymer backbone, affecting its mechanical and physical properties. A higher VA content decreases the polymer's melting point, stiffness, and crystallinity and increases its polarity, flexibility, and adhesion, resulting in a wide spectrum of applications. In the pharmaceutical field, the usage of EVA polymers covers different applications including transdermal drug delivery, intrauterine devices, and subcutaneous implants (Celanese, 2015a). EVA-based formulations were broadly studied as interesting candidates for 3D printing applications thanks to the advantageous features of this material, such as the versatility, the easy extrudability without the addition of any plasticizer, and the low glass transition (Samaro et al., 2021) (Almeida et al., 2011) (Schneider et al., 2017). Nevertheless, their compatibility with the DPE technique was poorly tested.

This study aimed to manufacture, for the first time, 3D-printed EVA-based transdermal patches with the DPE technique, given the consolidated utilization of this material in transdermal drug delivery systems (TDDS) as a rate-controlling membrane (Celanese, 2015a). Moreover, the versatility of EVA in preparing patches for personalized transdermal therapies was highlighted by selecting two model drugs with dissimilar melting

points. Specifically, EVA 1821A (18% VA) and EVA 4030AC (40% VA) were chosen to meet the characteristics of diclofenac sodium and ibuprofen respectively. The resulting printed products were physicochemically characterized using Fourier-transform infrared spectroscopy (FTIR), differential scanning calorimetry (DSC), and thermogravimetric analysis (TGA), to study the effect of EVA grade on the characteristics of the drug-loaded patches. Furthermore, their mechanical properties were evaluated with a texture analyzer (TA). Finally, the release and permeation profiles of the model drugs were determined with vertical diffusion cells mounting skin-mimicking membranes.

2. Materials and Methods

2.1 Materials

Both grades of ethylene vinyl acetate (EVA) copolymer (Ateva 4030AC and Ateva 1821A), in micronized form, were kindly donated by Celanese (Germany). Ibuprofen and diclofenac sodium were provided from BASF (Germany) and Farmalabor (Italy) respectively. Strat-M® membranes were purchased from Merck Millipore (USA). All the solvents used were analytical grade.

2.2 Methods

2.2.1 Direct 3D printing of drug-loaded transdermal patches

Mixtures of EVA 4030AC and ibuprofen (F1), and EVA 1821A and diclofenac sodium (F2) were used as feedstocks for subsequent 3D printing with direct powder extrusion. Each formulation was prepared by carefully weighing the model drug and the polymer, mixing them manually with a mortar and pestle, and then automatically using a powder blender (Galena Top, Ataena Srl, Italy). The defined ibuprofen and diclofenac sodium proportion was 30 % wt to load approximately 1 g of active compound into the 3D printed patch. The prepared blends (approximately 3.5 g each) were then directly added to the hopper of the DPE 3D printer (3D Cultures, USA), which was equipped with a single screw extruder with a nozzle diameter of 1 mm. Key parameters were optimized, including print speed, layer height, and printing temperature. The print speed was set at 10 mm/s and the layer height was 0.6 mm with 100 % of infill density. These print settings remained constant for both formulations. On the contrary, the printing temperature was set according to the drug contained in the formulation and the coupled polymer characteristics (80 °C for F1 and 180 °C for F2). In addition, to increase adhesion to the plate, the build plate was kept at 45 °C and covered with an adhesion sheet (Polypropylene, Ultimaker, The Netherlands). The patch geometry (side x height: 70x50 mm) was designed using computer-aided design (CAD) software (Tinkercad®, Autodesk, USA) to create an STL file format compatible with the Ultimaker Cura 4.1 Software (Ultimaker, The Netherlands).

2.2.2 Characterization of 3D printed transdermal patches

2.2.2.1 Thickness and weight uniformity

After the printing, the resulting patches were weighed, and their thicknesses were measured to evaluate the reproducibility of the printing process. Thickness measurements were performed using a digital caliper (Mitutoyo, Japan). Average thickness, weight, and standard deviation values were calculated from triplicate measurements.

2.2.2.2 Content uniformity

Six portions were cut from different sections of the printed patches, weighed, and placed in ethanol to assess the homogeneous distribution and the effective amount of ibuprofen and diclofenac sodium present in each patch. All the samples were shaken continuously for 24 hours at 100 rpm. Then, the amount of the drug was measured with high-performance liquid chromatography (HPLC, Agilent 1260 Infinity II, Agilent, USA). For HPLC analysis, the mobile phase consisted of a mixture of 0.5 % formic acid in water and acetonitrile (ratio 20:80) for ibuprofen, and a mixture of 0.5 % formic acid in water and methanol (ratio 30:70) for diclofenac sodium. The flow rate of the mobile phase was set at 1 mL/min, and a C18 (Agilent Poroshell 120, 150 x 4.6mm, 5 µm) column (Agilent, USA) was used for analysis. The injection volume was set at 20 µL and the detection signal was recorded at 220 nm for ibuprofen and 274 nm for diclofenac sodium, keeping the analysis system at room temperature.

2.2.2.3 Mechanical properties

The break strength and degree of flexibility of the drug-loaded and blank printed patches were explored using a texture analyzer (TA.XT plus Texture Analyzer, Stable Micro Systems, UK) (Donnelly et al., 2010) (Azizoğlu et al., 2020). A customized 3D printed apparatus was realized as support for attaching samples and was mounted on the working stage of the texture analyzer, as shown in Figure 1. For all measurements, the texture analyzer was set in compression mode and an aluminum probe (2.0 mm in thickness) was moved into the middle of the patch at a speed of 2 mm/s. Considering the maximum peak of the force-distance curve, we extrapolated the break strength of the 3DP patches. As regards the degree of flexibility of each sample, it was calculated as the angle (θ) of patch bending upon break (Box of Fig. 1). The tangent of the angle was calculated using equation 1, and the bending angle was calculated with the arctangent formula (Equation 1).

$$tan\theta = \frac{b}{a/2} \quad (1)$$

where a is the initial length of the patch, b is the distance traveled by the probe before the patch was broken and θ is the angle determined at the point when the patch was broken.

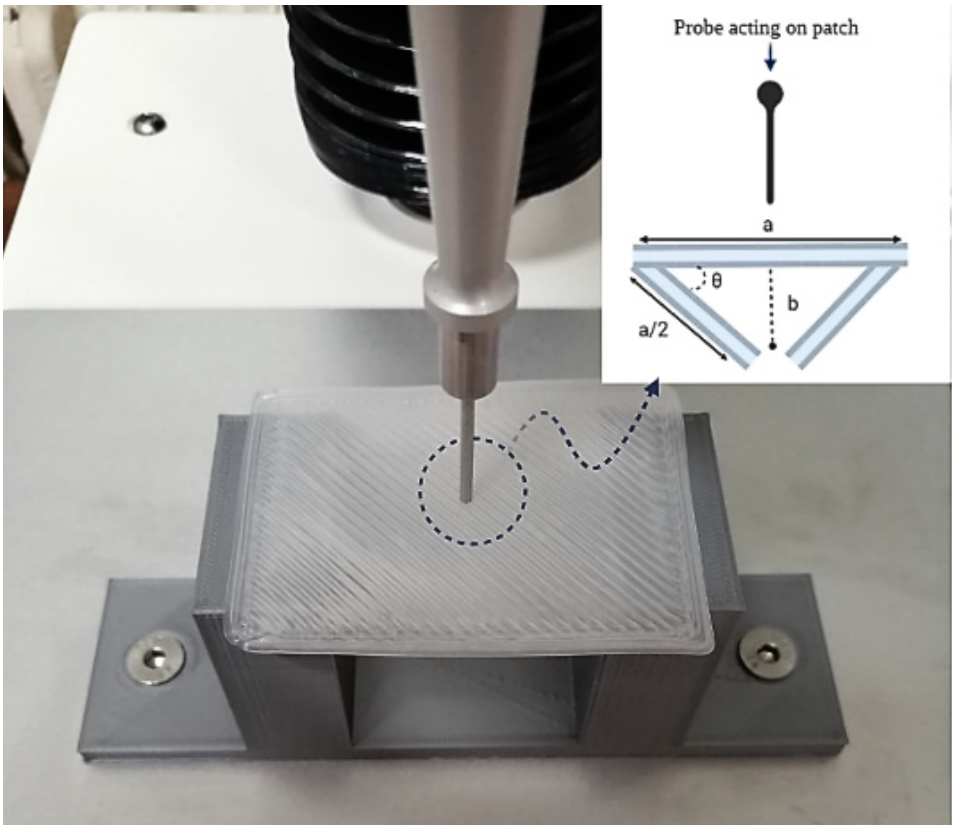

Figure 1. Image of mechanical analysis of a 3D printed patch with texture analyzer; Box: illustration of the method used to measure the degree of flexibility of the 3D printed patches.

2.2.2.4 Thermal analysis

The thermal behavior of pure starting materials (ibuprofen, diclofenac sodium, EVA 4030AC, and EVA 1821A) and printed formulations was investigated through differential scanning calorimetry (DSC 6000, Perkin Elmer, USA) and thermogravimetric analysis (TGA 4000, Perkin Elmer, USA). For TGA analysis, samples were equilibrated at 30 °C and heated up to 550 °C at a heating rate of 10 °C/min under a nitrogen flow rate of 30 mL/min, while recording the weight loss. DSC measurements were carried out by placing the samples (around 5 mg) in aluminum pans. Samples were heated up with a heating rate of 10 °C/min from 30 °C to 180 °C, hold for 3 min, then cooled down to -30 °C at 50 °C/min, hold for 3 min, and lastly, heated up again to 180 °C at 10 °C/min. Pyris Manager software (Perkin Elmer, USA) was used for data collection and analysis.

2.2.2.5 ATR-FTIR analysis

The structure analysis of raw materials and printed patches was conducted using attenuated total reflectance Fourier transformed infrared spectroscopy (ATR-FTIR, Spectrum Two FT-IR spectrometer with ATR

accessory, Perkin Elmer, MA, USA). The samples were scanned 64 times with the spectra resolution of 4 cm^{-1} at room temperature to obtain the ATR-FTIR spectra in a range of wave numbers from 4000 to 450 cm^{-1}.

2.2.3 In vitro drug release studies

The release profile of the printed patches was evaluated in a 50% (v/v) ethanolic phosphate buffer saline (PBS at pH= 7.4) solution. All patches were weighed and then immersed in sealed glass bottles containing 100 ml of release medium. The bottles were incubated at 37 °C under stirring (100 rpm) for 48 hours. At designated time points (1 h, 2 h, 4 h, 6 h, 24 h, and 48 h), 1 mL of release medium was taken out and replaced with an equal volume of the fresh one. The amount of ibuprofen and diclofenac sodium released from the patches was measured with HPLC as reported above. Triplicate measurements were made for each sample.

2.2.4 In vitro permeation studies

In *vitro* drug permeation studies were carried out using vertical diffusion cells (Franz cells) with a receptor compartment volume of 7 mL and an effective diffusion area of 1.766 cm^2. PBS (pH= 7.4) was used as receptor media and the receptor compartment was stirred continuously at 400 rpm by a magnetic stirrer. The system was thermostated at 32 ± 0.5 °C with a circulating jacket. A Strat-M® membrane was applied as the partitioning membrane. Strat-M® is a commercially available skin-mimic artificial membrane that comprises a tight top layer coated with a lipid blend and supported by two layers of polyethersulfone on top of one layer of polyolefin. This multi-layered structure allows the Strat-M® to simulate the morphology and the lipid chemistry of human skin (Haq et al., 2018). At defined sampling intervals (1 h, 2 h, 4 h, 6 h, 24 h, and 48 h), 0.2 ml of the receptor solution was withdrawn and replaced with an equal volume of fresh buffer. The amount of ibuprofen and diclofenac in all samples was then determined with HPLC as reported above. Triplicate measurements were made for each sample.

3. Results and discussion

3.1 Characterization of 3D printed patches

3.1.1 Morphology and physicochemical properties

DPE technique was successfully employed for the first time to produce EVA-based transdermal patches (Figure 2). EVA 4030AC and EVA 1821A were selected as polymeric matrices, thanks to their different physicochemical properties influenced by the percentage of vinyl acetate contained (40 % of VA and 18 % of VA respectively). Ibuprofen and diclofenac sodium were chosen as model drugs to demonstrate the adaptability of different EVA grades to drugs with significantly different thermal behavior to guarantee the printability of the desired patch. For this purpose, ibuprofen, which has melting and gradation temperatures much lower than those of diclofenac sodium, was printed in association with EVA 4030AC, which has a lower melting temperature than EVA 1821A. For the same reason, diclofenac sodium was printed in association with EVA 1821A.

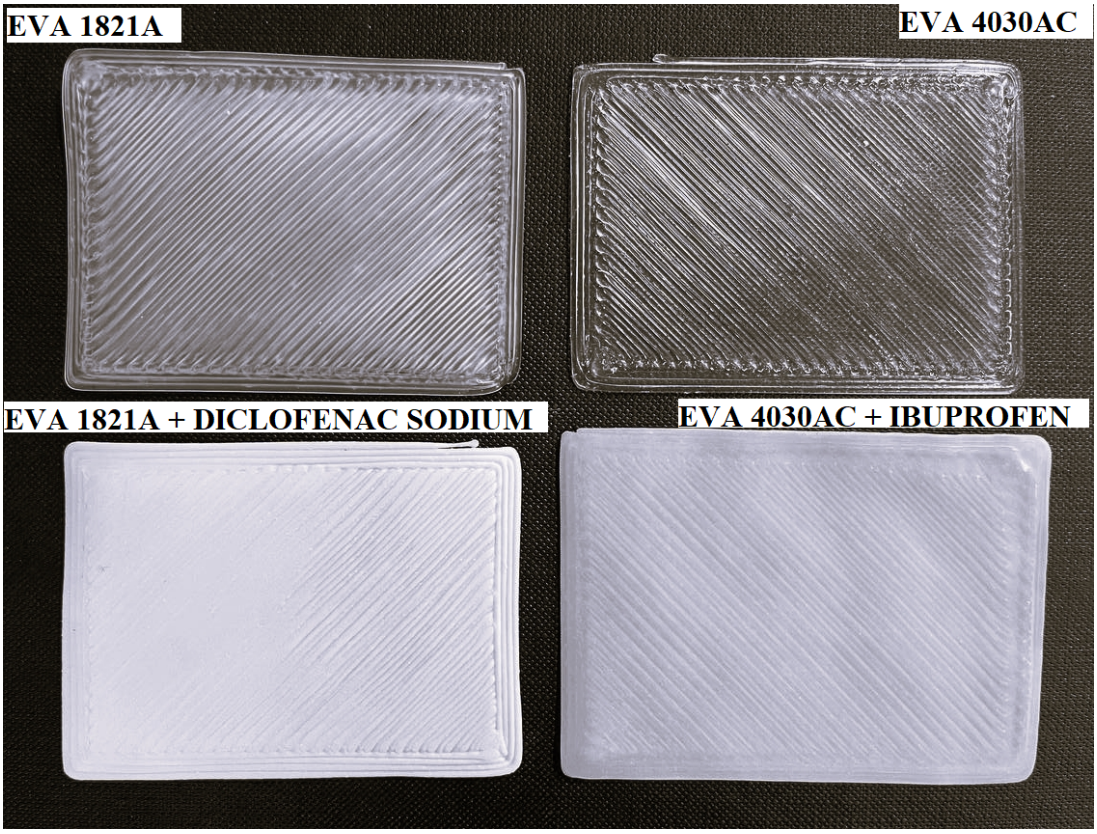

Figure 2. Top view of drug-loaded and blank EVA-based transdermal patches.

The resulting patches were weighed immediately after the printing and their thickness was measured at six different points using a digital caliper. All the printed patches of each batch did not show significant differences in weight and thickness as reported in Table 1, suggesting that the reproducibility of the printing process was achieved.

Table 1. Analysis of weight and thickness of produced patches.

Sample (patch)	Average weight (g)	Average thickness (mm)
EVA 4030AC	2,52 ± 0,13	0,80 ± 0,01
EVA 1821A	2,80 ± 0,11	1,10 ± 0,01
EVA 4030AC + Ibuprofen	3,62 ± 0,02	1,01 ± 0,01
EVA 1821A + Diclofenac sodium	3,25 ± 0,01	1,02 ± 0,02

The drug-loaded patches presented a whitish appearance compared with the transparent blank ones, due to the presence of the drug. EVA4030AC-based patches exhibited greater softness and transparency than those based on EVA 1821A according to the higher percentage of VA contained (Celanese, 2015b).

Furthermore, using a digital microscope (Pancellent, China), no visible particles were observed within the printed formulations (Figure 3), indicating that the pure components were well-mixed and uniformly distributed in the patches. Even the individual layers of the patches were symmetrical from the microscope images, confirming the good printability of the mixtures.

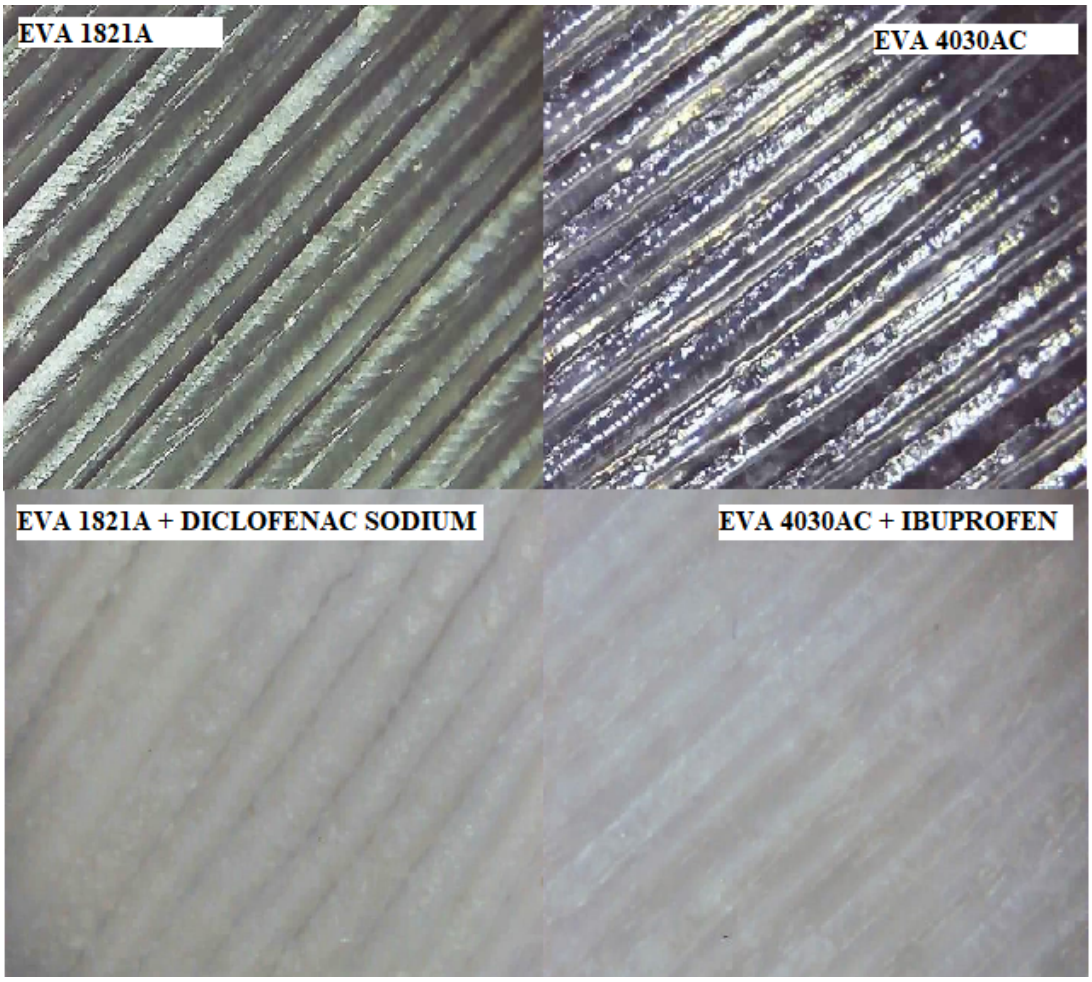

Figure 3. Microscope images of drug-loaded and blank EVA-based transdermal patches.

3.1.2 Content uniformity

The homogeneous distribution and the effective amount of ibuprofen and diclofenac sodium present in the samples were evaluated by cutting, weighing, and placing in ethanol different pieces of the drug-loaded patches. A HPLC measured the amount of drug dissolved in ethanol after 24 hrs. EVA 4030AC-based patches contained 74.6 ± 0.9 mg/g of ibuprofen proving an effective drug loading of 22.4 %. EVA 1821A-based patches contained 23.3 ± 0.7 mg/g of diclofenac sodium proving an effective drug loading of 7 %. Therefore, considering the average weight of drug-loaded printed patches (Table 1) the effective amount of ibuprofen and diclofenac was respectively 811 mg and 228 mg for one patch (Tiboni et al., 2021). The printed patches proved to have a homogeneous distribution of the drug within them, but the effective amount of diclofenac sodium loaded was much lower than that of ibuprofen. This can probably be explained by the better flowability of the mixture of ibuprofen and EVA 4030AC compared to the one of diclofenac sodium and EVA 1821A during the printing process.

3.1.3 Break strength and degree of flexibility

The mechanical properties of produced 3D printed patches were evaluated with a texture analyzer. Flexibility tests were conducted on both drug-loaded and blank patches to ensure that these do not break during transport and use. The degree of flexibility was considered as the angle (θ) of patch bending upon break, while the value of break strength was extrapolated from the maximum peak of the force-distance curve. These calculated parameters are reported in Table 2. All samples showed a good degree of flexibility since they could bend to more than 60 °, and the addition of ibuprofen and diclofenac sodium did not significantly affect the flexibility of the samples (Azizoğlu et al., 2020). Moreover, EVA 4030AC-based patches were broken after applying less strength than was needed to break EVA 1821A-based patches due to the lower hardness of the polymer.

Table 2. Maximum bending angles and break strengths of 3D printed patches.

Sample (patch)	**Break strength (N)**	**Degree of flexibility (θ °)**
EVA 4030AC	5,7 ± 0,1	67,3 ° ± 0,5
EVA 1821A	31,7 ± 0,2	67,1 ° ± 0,5
EVA 4030AC + Ibuprofen	8,3 ± 0,1	61,2 ° ± 0,2
EVA 1821A + Diclofenac sodium	24 ± 0,1	67,5 ° ± 0,3

3.1.4 Thermal behavior

Thermal analyses were performed on pure materials to assess their melting and degradation temperatures and choose the most appropriate EVA grade for each model drug. As well the effect of drugs on the thermal behavior of EVAs after the printing process was investigated. The thermograms of pure materials and printed formulations are shown in Figure 4, and their melting temperatures are reported in Table 3. Considering the thermograms of model drugs, ibuprofen melted at 78 °C while diclofenac sodium did not melt in the temperature range chosen for the analysis. Indeed, the endothermic peak at about 56°C is probably due to the water evaporation from the surface of the drug (Arany et al., 2020) (Figure 4B) since this peak disappears in the second heating scan (Supplementary figure DSC-S1b).

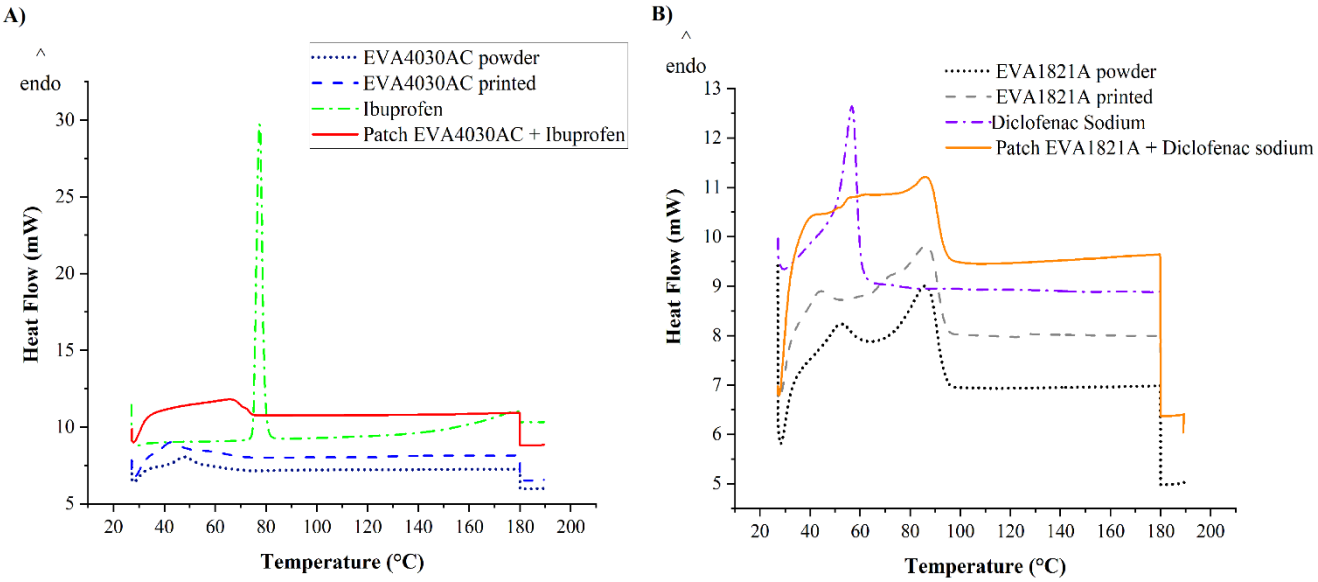

Figure 4. DSC thermograms of the pure materials and 3D printed formulations.

EVA 1821A powder showed a double melting peak (Tm_1= 52 °C and Tm_2= 86 °C) indicating that this grade of the polymer contains two different types of crystals (polymorphs) in its structure (Almeida et al., 2011) (Genina et al., 2016). In the printed EVA1821A, the first peak fell at a lower temperature of 44°C; while the second peak changed to a broad shoulder with the T_m at 71°C, followed by the peak at 86°C (Fig. 4B). Since the thicker the crystal, the higher the melting temperature (Stark et al., 2011), both the melting temperature depression, as well as the presence of the new shoulder, could be attributed to the distribution of crystals with reduced thickness, because of the thermal treatment followed by rapid cooling during printing. This hypothesis is supported by the disappearance of the lower temperature peak and the shoulder in the second heating scan carried out after a controlled cooling (Supplementary figure DSC-S1b). Indeed, the controlled cooling allowed the polymer to crystallize into thicker crystals, typical of the starting powder.

For the aforementioned reason, EVA 1821A was chosen in association with diclofenac sodium to avoid the alteration of the drug during the extrusion and low morphological quality of the printed products.

The DSC trace of the EVA 1821A with diclofenac showed the same endothermic peak of the printed EVA, suggesting that the drug did not modify the crystalline structure of the polymer (Fig. 4B).

EVA 4030AC powder had a net melting peak at 48°C which shifted at a lower temperature of 42°C in the printed polymer (Fig. 4A). Even in this case, the lowering of the melting peak could be attributed to the presence of smaller crystals formed during rapid cooling. Indeed, the second heating scan carried out after the controlled cooling of the polymer showed only one melting peak at 48°C related to crystals typical of the starting powder (Supplementary figure DSC-S1a).

For this reason, EVA 4030AC was chosen in association with ibuprofen for 3D printing to avoid the alteration of the drug during the extrusion and low morphological quality of the printed products.

Compared to the printed EVA, the patch of EVA4030AC loaded with ibuprofen showed a broad peak shifted to a higher temperature of 67°C followed by a shoulder at 72°C (Fig. 4A). There is no significant difference in the T_m of the EVA 4030AC melting peaks in the drug-free and drug-loaded patches. Therefore, the widening of this melting peak and the shift to higher temperatures could be due to a merge between the EVA melting peak and the ibuprofen melting peak, which shifted to a lower temperature after printing. The depression of the melting point of ibuprofen after printing could be attributed to the dissolution of the drug into the polymer matrix to some extent (Genina et al., 2016).

The samples' crystallinity degree (χ) was calculated according to equation 2 and tabulated in Table 3.

$$\chi\,(\%) = [\frac{\Delta H_f}{\left(\Delta H_f^* * \Delta EVA\right)} * 100] \quad (2)$$

where ΔH_f is the melting enthalpy of the analyzed EVA samples, ΔH_f^* is the tabulated melting enthalpy of the perfect polyethylene (PE) crystal ($\Delta H_f^* = 277.1\,J/g$), and ΔEVA is the weight fraction of EVA in the sample (Shi et al., 2008).

The degree of crystallinity of analyzed EVA powders and printed EVAs decreased as the VA content increased, since the VA-comonomer reduced the stereoregularity in the polymer chains, generating a decrease in the crystallinity of the PE segments (Wang et al., 2019). The higher crystallinity of printed EVA 1821A compared to the powder could be attributed to the formation of crystals with reduced thickness causing a melting peak broadening. Therefore, the calculated crystallinity degree refers to all crystalline forms characterizing the printed polymer. Finally, in the drug loaded patches, particularly in the one loaded with ibuprofen, it was difficult to establish the degree of crystallinity of the EVA polymer since the melting peak of the drug, shifted to a lower temperature after printing, merged with that of the polymer.

Table 3. Main parameters obtained from the thermal analysis of the samples.

Sample	$Tm_1\ (°C)$	$Tm_2\ (°C)$	**χ (%)**	$T_{onset}\ (°C)$	$T_d\ (°C)$
EVA 4030AC powder	48	-	2	417	471
EVA 1821A powder	52	86	10	426	473
EVA 4030AC printed	42	-	2	-	-
EVA 1821A printed	44	86	14	-	-
EVA 4030AC + Ibuprofen	67	-	-	418	471

EVA 1821A + Diclofenac sodium	42	87	-	439	482
Ibuprofen	78	-	-	176	236
Diclofenac sodium	-	-	-	282	311

Concerning the thermal stability of the samples, TGA analyses (Figure 5A, B) were carried out to ensure the safe use of the selected drugs for 3D printing. The onset temperatures (T_{onset}) and the temperatures related to the maximum degradation rate (T_d) were calculated through DTG (Figure 5C, D) and are presented in Table 3. Both model drugs proved to stay stable at processing temperature with a weight loss of approximately 2% at 176 °C for ibuprofen and 283 °C for diclofenac sodium. Pure EVAs presented two weight losses: a small degradation phase at a lower temperature (T_{onset} of 319 °C with a T_d of 352 °C for EVA 4030AC and T_{onset} of 328 °C with a T_d of 364 °C for EVA 1821A) which is due to acetic acid loss and the main degradation phase at a higher temperature (T_{onset} of 417 °C with a T_d of 471 °C for EVA 4030AC and T_{onset} of 426 °C with a T_d of 473 °C for EVA 1821A) which is due to fragments of the polymer backbone (Díez et al., 2021). EVA-based loaded patches degraded with the same trend as pure EVAs and at approximately the same temperatures, demonstrating that drugs did not reduce the thermal stability of the polymers.

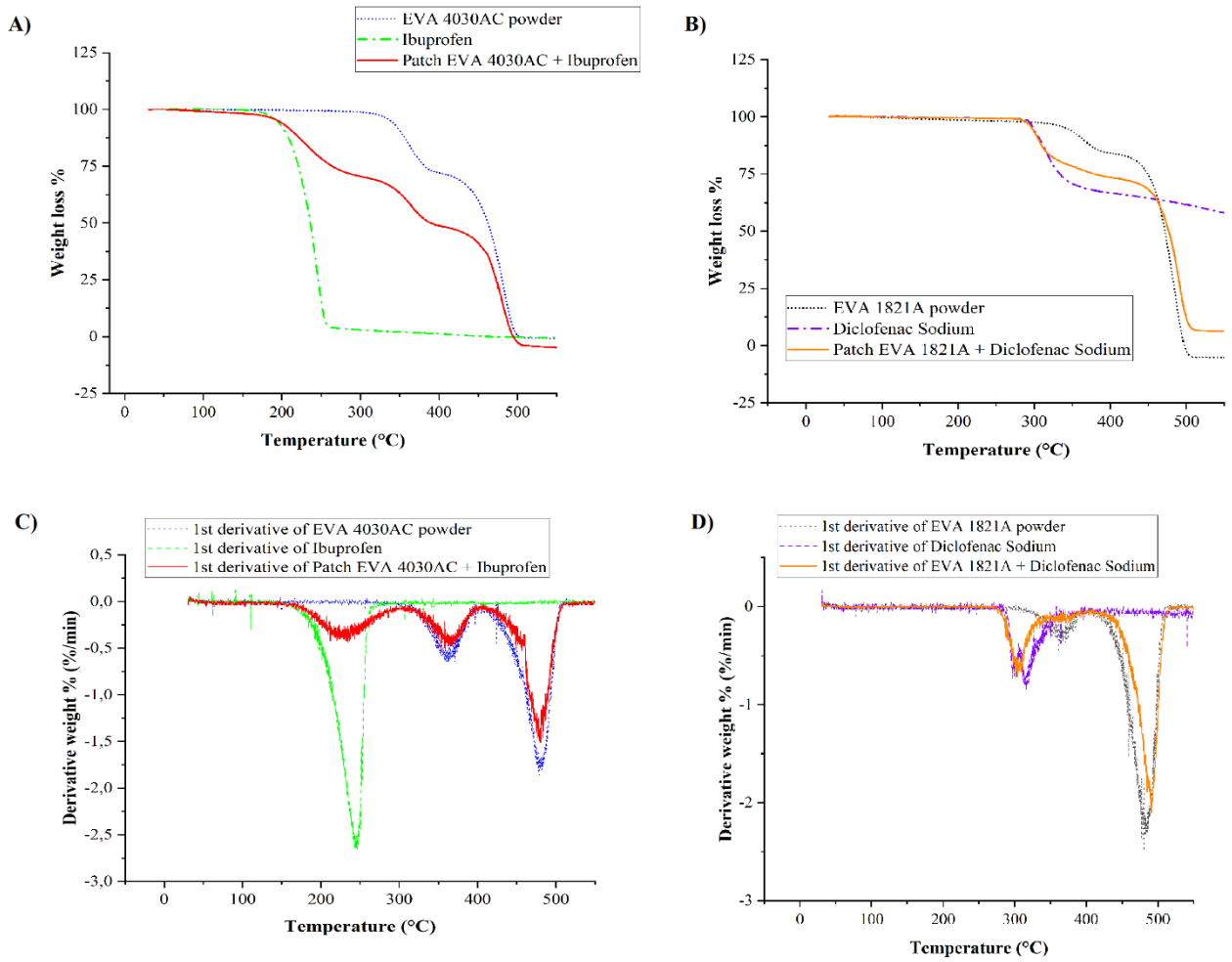

Figure 5. A) TGA and C) DTG of pure ibuprofen, pure EVA 4030AC and EVA 4030AC/ibuprofen printed patch; B) TGA and D) DTG of pure diclofenac sodium, pure EVA 1821A and EVA 1821A/diclofenac sodium printed patch.

3.1.5 Investigation of chemical characteristics through ATR-FTIR spectroscopy

ATR-FTIR analyses were conducted to obtain further information on the chemical composition of 3D printed patches and to investigate whether interactions between the polymer and drug had occurred. FTIR spectra of pure materials and 3D printed formulations are compared in Figure 6.

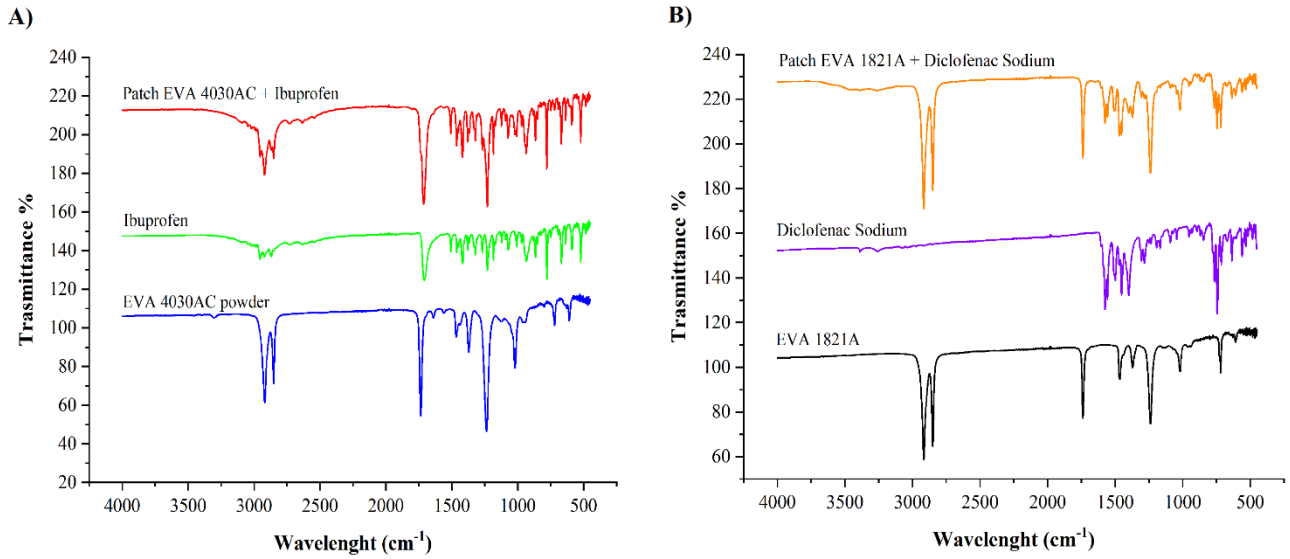

Figure 6. Comparison of FTIR spectra of A) pure Ibuprofen, pure EVA 4030AC, and EVA 4030AC/Ibuprofen printed patch and B) pure Diclofenac sodium, pure EVA 1821A, and EVA 1821A/Diclofenac sodium printed patch.

As it can be observed, both spectra of 3D printed patches presented the characteristic peak of EVA polymer at 1737 cm^{-1} related to a carbonyl C═O stretching (Genina et al., 2016). The spectrum of the printed EVA 4030AC/Ibuprofen patch showed the absorption band of C=O and OH functional groups of ibuprofen at 1714 cm^{-1} and 2995 cm^{-1} respectively (Elkordy et al., 2010). The spectrum of the printed EVA 1821A/Diclofenac sodium patch showed the absorption band of C═C, OH, and NH functional groups of diclofenac sodium at 1575 cm^{-1}, 3260 cm^{-1}, and 3387 cm^{-1} respectively (Swain et al., 2015). This suggested that both the polymer and drug were effectively incorporated into the final formulations. No new chemical bonds were established for EVA during the printing process since the spectra of the pure materials and final formulations were found to be similar. Moreover, the homogeneous distribution of the drug within the printed devices was evaluated by analyzing random portions of the samples with FTIR. The resulting spectra were normalized with the EVA absorption at 1737 cm^{-1} as a reference and reported in Figure 7 (Moroni et al., 2022). In agreement with content uniformity analysis, the printed patches proved to have a homogeneous composition considering that no notable differences in the intensities of the characteristic peaks of the drugs were found.

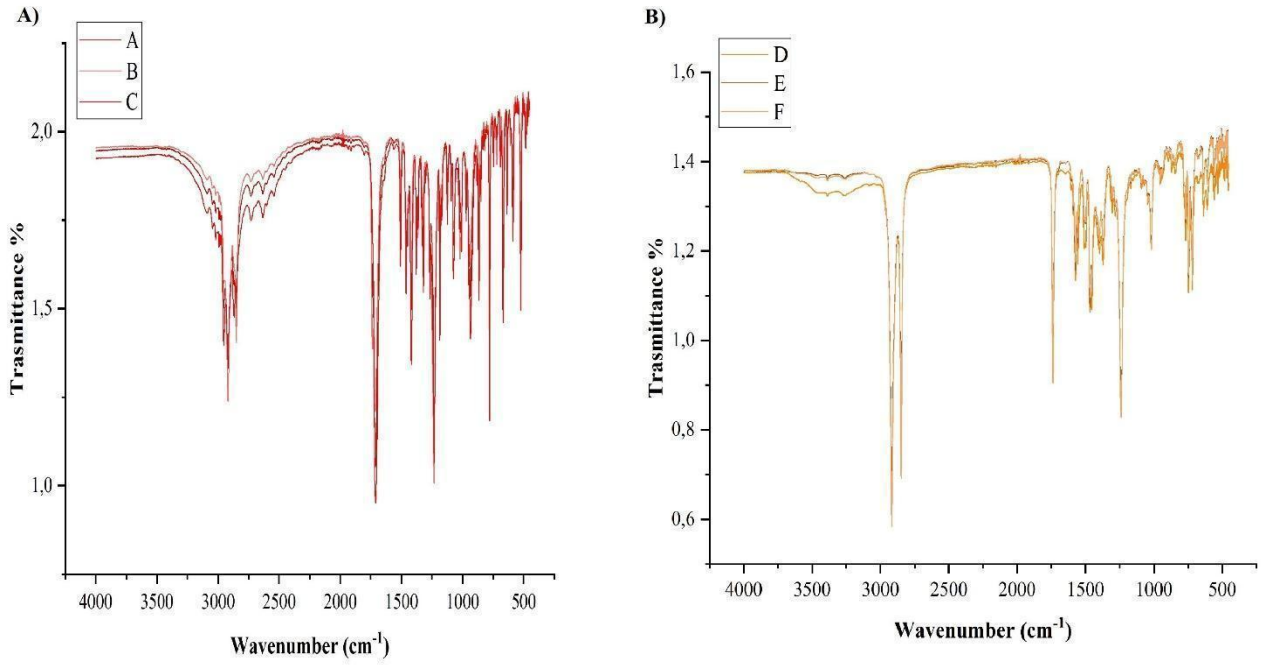

Figure 7. Composition homogeneity of A) EVA 4030AC/Ibuprofen printed patches and B) EVA 1821A/Diclofenac sodium printed patches.

3.1.6 In vitro Ibuprofen and Diclofenac sodium release and permeation profiles

Drug release from 3D printed patches was tested in a mixture of 50% ethanol in PBS (pH = 7.4) considering the poor solubility of the model drugs in water. Figure 8 illustrates the cumulative percentage of ibuprofen and diclofenac sodium released from EVA patches over a period of 48 hrs.

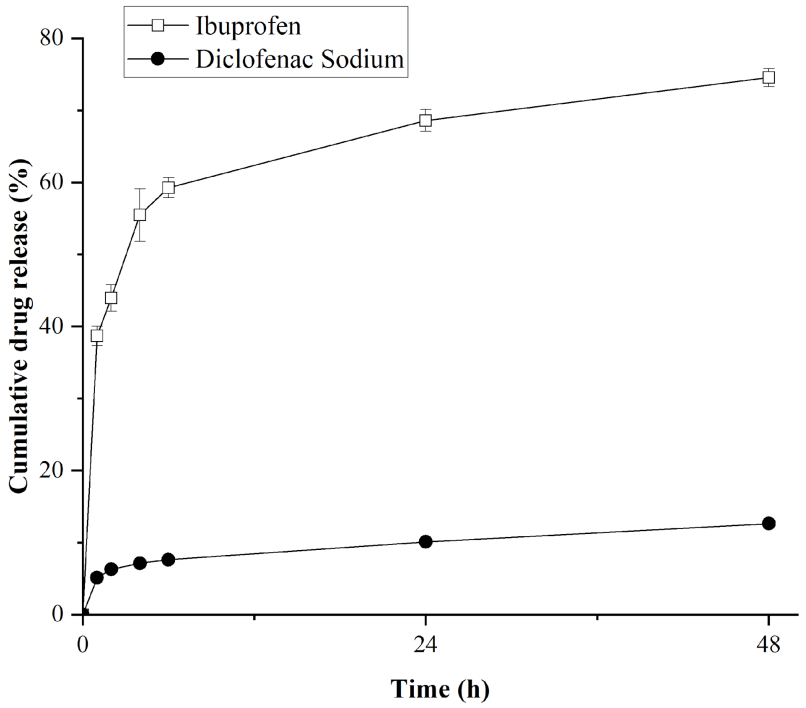

Figure 8. In vitro release profiles of Ibuprofen and Diclofenac sodium from EVA 4030AC and EVA 1821A-based patches respectively. All values are presented as mean ± SD, where n = 3.

Both formulations exhibited an initial burst release phase in the first 6 hrs more pronounced for ibuprofen than for diclofenac sodium and followed by a steady release phase. The initial fast release might be contributed by the instantaneous dissolution of surface-bound drug molecules in the release medium (Tang et al., 2010), while the subsequent slowing of the release rate is probably attributed to the diffusion of drug molecules through the polymer matrix. The cumulative release of ibuprofen was 366.65 mg and that of diclofenac sodium was 49.26 mg after 48 hrs (74.5% and 12.6% of the total amount present in one patch respectively). These results are consistent with previous studies (Tallury et al., 2007) (Shin et al., 2002) which demonstrated that the vinyl acetate content of EVA copolymer affected the drug release rate. An increase in permeability of the polymer and a consequent increase in the release rate was observed with an increment in VA content, as the introduction of amorphous VA comonomer to a highly crystalline polyethylene decreases the crystallinity of the system and improves the microporosity of the whole matrix (Kamath et al., 1965). Effectively, DSC analyses confirmed that EVA 1821A possesses a higher crystalline structure than EVA 4030AC. In this way, by varying the grade of EVA copolymer the drug's permeation rate through EVA membranes can be controlled, representing an important advantage for personalized transdermal therapies.

Furthermore, to clarify the kinetics of ibuprofen and diclofenac sodium release from EVA patches the data obtained from release profiles were fitted by Korsmeyer-Peppas (equation 3) and Peppas-Sahlin (equation 4) models.

$$\frac{M_t}{M_\infty} = kt^n \quad (3)$$

$$\frac{M_t}{M_\infty} = K_d t^m + K_r t^{2m} \quad (4)$$

where $\frac{M_t}{M_\infty}$ is a fraction of drug released at time t, k is the release rate constant, n is the release exponent, K_d is the diffusion constant, K_r is the relaxation constant, and m is the Fickian diffusion exponent (Mehran et al., 2020).

The correlation coefficients (R^2) and constants of each model are shown in Table 4, and the release data fitting to each model are shown in Figure 9. Considering the correlation coefficient (R^2) both models well described the release kinetics of ibuprofen (0.987, 0.954) and diclofenac sodium (0.995, 0.944). In the Korsmeyer-Peppas model, the n values less than 0.5 reflected a quasi-Fickian diffusion mechanism which indicates the drug release through non-swellable matrix diffusion (Paarakh et al., 2018). Moreover, to determine the predominant mechanism among drug diffusion and polymer relaxation, the drug release profile of all formulations was fitted to the Peppas-Sahlin equation. The higher value of K_d than K_r indicates that Fickian diffusion was the predominant mechanism of drug release from the matrices than polymer relaxation and swelling in such matrix (Baggi et al., 2016).

Table 4. Kinetics parameters of drug release studies.

	Korsmeyer-Peppas			**Peppas-Salhin**		
Drug	**k**	**n**	R^2	$K_d(h^{-0.45})$	$K_r(h^{-0.45})$	R^2
Ibuprofen	42 ± 2	0.15 ± 0.02	0.987	36 ± 2	-4.1 ± 0.5	0.954
Diclofenac Sodium	5.2 ± 0.1	0.22 ± 0.01	0.995	4.5 ± 0.4	-0.42 ± 0.08	0.944

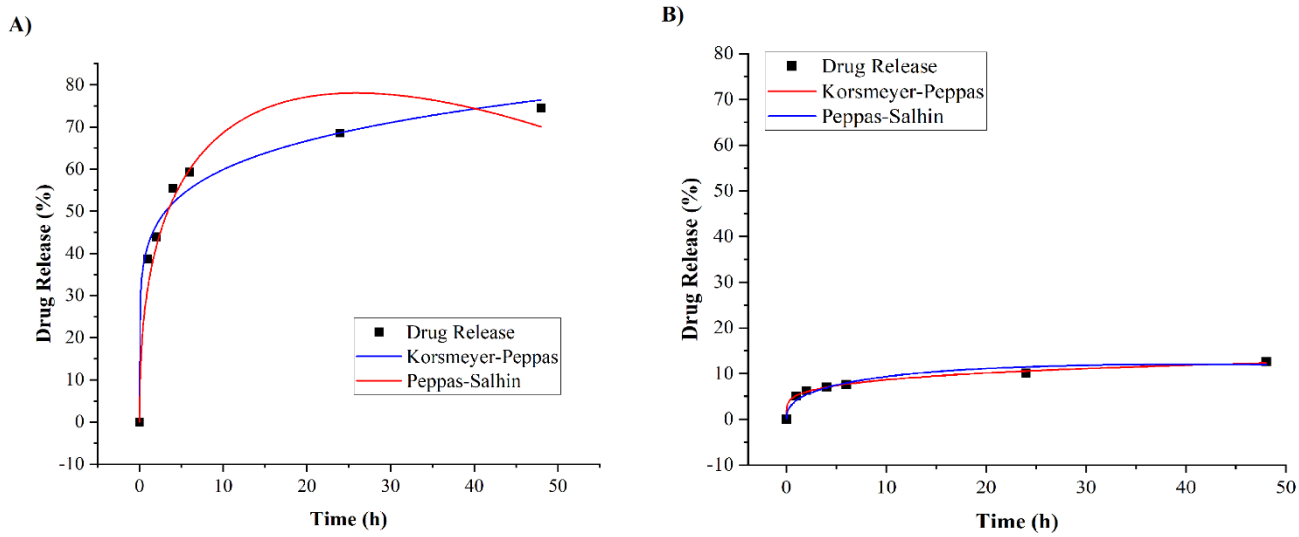

Figure 9. Release data of A) Ibuprofen and B) Diclofenac sodium fitting to Korsmeyer-Peppas and Peppas-Salhin models.

Additionally, the in *vitro* ibuprofen and diclofenac sodium permeation behavior was determined using vertical diffusion cells. An artificial Strat-M® membrane was selected as the partitioning membrane since it was reported to have comparable results to human skin (Haq et al., 2018). The *in vitro* permeation profiles represented in Figure 10 indicate that ibuprofen reached a higher permeation (642.1 µg/cm²) compared to the diclofenac sodium (394.22 µg/cm²) over the 48 hrs of experimentation. These results are consistent with that of release studies where it was found that the EVA 4030AC-based patch possessed a fast release behavior while the one based on EVA 1821A had a sustained release behavior. Moreover, previous findings (Pradal, 2020) revealed that ibuprofen permeates through human skin to a greater extent than diclofenac sodium due to its lower molecular weight and higher pKa value which affect in part the drug permeation rate.

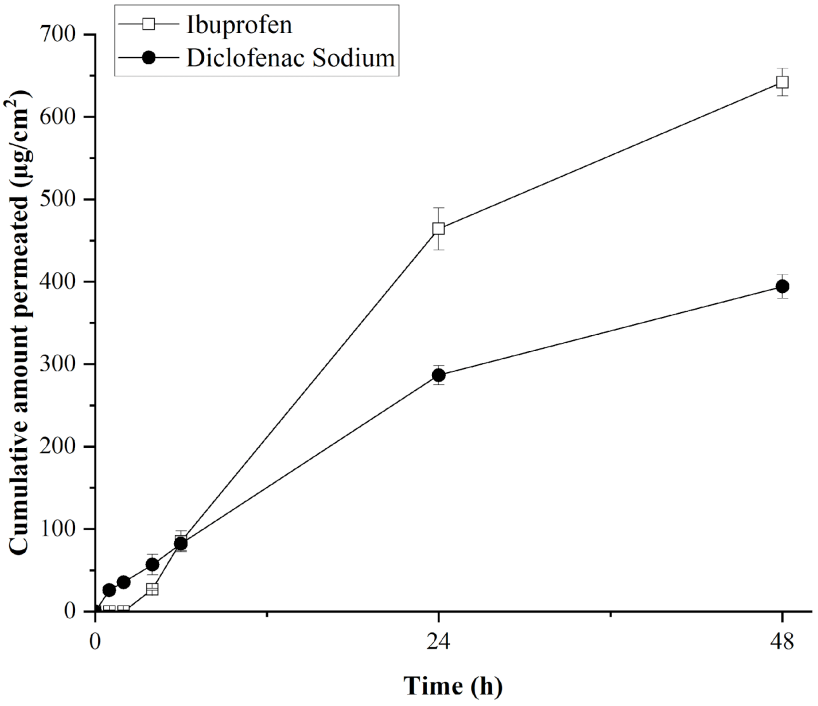

Figure 10. In vitro permeation profiles of Ibuprofen and Diclofenac sodium through Strat-M® membrane from EVA 4030AC and EVA 1821A-based patches respectively. All values are presented as mean ± SD, where n = 3.

4. Conclusions

This work demonstrated, for the first time, the application of EVA and 3DP-DPE as potential tools for manufacturing transdermal patches that can be customized according to the patient's needs, thanks to the polymer's tailorable properties and compatibility with different drugs. Both chosen formulations showed excellent processability via the DPE technique, ensuring the thermal stability of the active compounds and good morphological quality of the extrudates. 3D-printed transdermal patches also exhibited adequate flexibility which prevents breakage during transport and use. Moreover, the VA content of the polymer played an important role in the permeability of the extruded EVA matrices, allowing that desired release and permeation profiles of the drug can be achieved with proper modifications. Therefore, by coupling the versatile physicochemical and mechanical properties of EVA excipient and the easy of use of DPE technology, it is believed that the 3D-printed EVA-based transdermal patches can be scalable for a potential practical application in pharmacies and hospitals.

Credit authorship

Giorgia Maurizii: Methodology, Investigation, Formal analysis, Data curation, Writing - original draft.

Sofia Moroni: Methodology, Investigation, Data curation.

Shiva Khorshid: Investigation, Data curation.

Annalisa Aluigi: Methodology, Data curation, Writing - review & editing.

Mattia Tiboni: Conceptualization, Supervision, Methodology, Formal analysis, Data curation, Writing - review & editing

Luca Casettari: Conceptualization, Resources, Funding acquisition, Project administration, Supervision, Writing - review & editing.

Conflict of interest

The authors declare no conflict of interest

Funding

Sofia Moroni acknowledge Marche Region for the PhD scholarship (Innovative doctoral programme POR Marche FSE 2014/2020 D.R. 354/2020).

This research received funding from Regione Marche (Italy) POR MARCHE FESR 2014–2020 - Asse 1 – OS 2 – Azione 2.1 https://www.marchebiobank.it.

Acknowledgments

We would like to express our sincere gratitude to Celanese for their contribution to this research and for providing Celanese EVA (ethylene vinyl acetate) used in this study as well as the support to article review. Moreover, we acknowledge ITIS E. Mattei (Urbino, PU, Italy) for the utilization of FT-IR instrument.

References

Almeida, A., Possemiers, S., Boone, M. N., De Beer, T., Quinten, T., Van Hoorebeke, L., Remon, J. P., & Vervaet, C. (2011). Ethylene vinyl acetate as a matrix for oral sustained release dosage forms produced via hot-melt extrusion. *European Journal of Pharmaceutics and Biopharmaceutics*, *77*(2), 297–305. https://doi.org/10.1016/j.ejpb.2010.12.004

Annaji, M., Ramesh, S., Poudel, I., Govindarajulu, M., Arnold, R. D., Dhanasekaran, M., & Babu, R. J. (2020). Application of extrusion-based 3D printed dosage forms in the treatment of chronic diseases. *Journal of Pharmaceutical Sciences*, *109*(12), 3551–3568. https://doi.org/10.1016/j.xphs.2020.09.042

Arany, P., Papp, I., Zichar, M., Csontos, M., Elek, J., Regdon, G., Budai, I., Béres, M., Gesztelyi, R., Fehér, P., Ujhelyi, Z., Vasvári, G., Haimhoffer, Á., Fenyvesi, F., Váradi, J., Miklós, V., & Bácskay, I. (2020). In vitro tests of FDM 3D-printed diclofenac sodium-containing implants. *Molecules*, 25(24), 5889. https://doi.org/10.3390/molecules25245889

Azizoğlu, E., & Özer, Ö. (2020). Fabrication of montelukast sodium loaded filaments and 3D printing transdermal patches onto packaging material. *International Journal of Pharmaceutics*, *587*, 119588. https://doi.org/10.1016/j.ijpharm.2020.119588

Baggi, R. B., & Kilaru, N. B. (2016). Calculation of predominant drug release mechanism using Peppas-Sahlin model, part-I (substitution method): A linear regression approach. Asian Journal of Pharmacy and Technology, 6(4), 223. https://doi.org/10.5958/2231-5713.2016.00033.7

Borandeh, S., van Bochove, B., Teotia, A., & Seppälä, J. (2021). Polymeric drug delivery systems by additive manufacturing. *Advanced Drug Delivery Reviews*, *173*, 349–373. https://doi.org/10.1016/j.addr.2021.03.022

Celanese, 2015a. Potential use of ethylene vinyl acetate copolymer excipient in Oral Controlled Release Applications: A literature review. https://explore.celanese.com/eva-in-oral-controlled-release-whitepaper-download (accessed October 6, 2022).

Celanese, 2015b. Injection molding guide for LDPE and Eva Copolymers. https://automotive.celanese.com/-/media/EVA-Polymers/Files/Product-Technical-Guides/EVA-016-PlasticsMoldingGuide-TG-EN-1115.pdf (accessed October 6, 2022).

Donnelly, R. F., Majithiya, R., Singh, T. R., Morrow, D. I., Garland, M. J., Demir, Y. K., Migalska, K., Ryan, E., Gillen, D., Scott, C. J., & Woolfson, A. D. (2010). Design, optimization and characterisation of polymeric microneedle arrays prepared by a novel laser-based micromoulding technique. *Pharmaceutical Research*, *28*(1), 41–57. https://doi.org/10.1007/s11095-010-0169-8

Durga Prasad Reddy, R., & Sharma, V. (2020). Additive Manufacturing in Drug Delivery Applications: A Review. *International Journal of Pharmaceutics*, *589*, 119820. https://doi.org/10.1016/j.ijpharm.2020.119820

Díez, E., Rodríguez, A., Gómez, J. M., & Galán, J. (2021). Tg and DSC as tools to analyse the thermal behaviour of Eva Copolymers. *Journal of Elastomers & Plastics*, *53*(7), 792–805. https://doi.org/10.1177/0095244320988163

Elkordy, A.A., & Ebtessam, A. (2010). Dissolution of Ibuprofen from spray dried and spray chilled particles. *Pakistan Journal of Pharmaceutical Sciences*, 23(3), 284-290.

Fanous, M., Gold, S., Muller, S., Hirsch, S., Ogorka, J., & Imanidis, G. (2020). Simplification of fused deposition modeling 3D-Printing Paradigm: Feasibility of 1-step direct powder printing for immediate release dosage form production. *International Journal of Pharmaceutics*, *578*, 119124. https://doi.org/10.1016/j.ijpharm.2020.119124

Genina, N., Holländer, J., Jukarainen, H., Mäkilä, E., Salonen, J., & Sandler, N. (2016). Ethylene vinyl acetate (EVA) as a new drug carrier for 3D printed medical drug delivery devices. *European Journal of Pharmaceutical Sciences*, *90*, 53–63. https://doi.org/10.1016/j.ejps.2015.11.005

Goyanes, A., Allahham, N., Trenfield, S. J., Stoyanov, E., Gaisford, S., & Basit, A. W. (2019). Direct powder extrusion 3D printing: Fabrication of drug products using a novel single-step process. *International Journal of Pharmaceutics*, *567*, 118471. https://doi.org/10.1016/j.ijpharm.2019.118471

Haq, A., Goodyear, B., Ameen, D., Joshi, V., & Michniak-Kohn, B. (2018). Strat-M® synthetic membrane: Permeability comparison to human cadaver skin. *International Journal of Pharmaceutics*, *547*(1-2), 432–437. https://doi.org/10.1016/j.ijpharm.2018.06.012

Kamath, P. M., & Wakefield, R. W. (1965). Crystallinity of ethylene–vinyl acetate copolymers. *Journal of Applied Polymer Science*, *9*(9), 3153–3160. https://doi.org/10.1002/app.1965.070090919

Mehran, M., Masoum, S., & Memarzadeh, M. (2020). Microencapsulation of Mentha spicata essential oil by spray drying: Optimization, characterization, release kinetics of essential oil from microcapsules in food models. *Industrial Crops and Products*, *154*, 112694. https://doi.org/10.1016/j.indcrop.2020.112694

Moroni, S., Khorshid, S., Aluigi, A., Tiboni, M., & Casettari, L. (2022). Poly(3-hydroxybutyrate): A potential biodegradable excipient for direct 3D printing of Pharmaceuticals. *International Journal of Pharmaceutics*, *623*, 121960. https://doi.org/10.1016/j.ijpharm.2022.121960

Paarakh, M.P., Jose, P.A., Setty, C.M., & Christoper., G.V.P. (2018). Release Kinetics-Concepts and Applications. *International Journal of Pharmacy Research & Technology*, 8(1), 12-20.

Pistone, M., Racaniello, G. F., Arduino, I., Laquintana, V., Lopalco, A., Cutrignelli, A., Rizzi, R., Franco, M., Lopedota, A., & Denora, N. (2022). Direct cyclodextrin-based powder extrusion 3D printing for one-step production of the BCS class II model drug niclosamide. *Drug Delivery and Translational Research*, *12*(8), 1895–1910. https://doi.org/10.1007/s13346-022-01124-7

Pradal, J. (2020). Comparison of skin permeation and putative anti-inflammatory activity of commercially available topical products containing ibuprofen and diclofenac. *Journal of Pain Research*, *Volume 13*, 2805–2814. https://doi.org/10.2147/jpr.s262390

Samaro, A., Shaqour, B., Goudarzi, N. M., Ghijs, M., Cardon, L., Boone, M. N., Verleije, B., Beyers, K., Vanhoorne, V., Cos, P., & Vervaet, C. (2021). Can filaments, pellets and powder be used as feedstock to produce highly drug-loaded ethylene-vinyl acetate 3D printed tablets using extrusion-based additive

manufacturing? *International Journal of Pharmaceutics*, *607*, 120922. https://doi.org/10.1016/j.ijpharm.2021.120922

Sánchez-Guirales, S. A., Jurado, N., Kara, A., Lalatsa, A., & Serrano, D. R. (2021). Understanding direct powder extrusion for fabrication of 3D printed personalised medicines: A case study for nifedipine minitablets. *Pharmaceutics*, *13*(10), 1583. https://doi.org/10.3390/pharmaceutics13101583

Schneider, C., Langer, R., Loveday, D., & Hair, D. (2017). Applications of ethylene vinyl acetate copolymers (EVA) in Drug Delivery Systems. *Journal of Controlled Release*, *262*, 284–295. https://doi.org/10.1016/j.jconrel.2017.08.004

Seoane-Viaño, I., Trenfield, S. J., Basit, A. W., & Goyanes, A. (2021). Translating 3D printed pharmaceuticals: From hype to real-world clinical applications. *Advanced Drug Delivery Reviews*, *174*, 553–575. https://doi.org/10.1016/j.addr.2021.05.003

Shi, X. M., Zhang, J., Jin, J., & Chen, S. J. (2008). Non-isothermal crystallization and melting of ethylene-vinyl acetate copolymers with different vinyl acetate contents. *Express Polymer Letters*, *2*(9), 623–629. https://doi.org/10.3144/expresspolymlett.2008.75

Shin, S. C., & Lee, H.-J. (2002). Controlled release of triprolidine using ethylene-vinyl acetate membrane and Matrix Systems. *European Journal of Pharmaceutics and Biopharmaceutics*, *54*(2), 201–206. https://doi.org/10.1016/s0939-6411(02)00051-6

Stark, W., & Jaunich, M. (2011). Investigation of ethylene/vinyl acetate copolymer (EVA) by Thermal Analysis DSC and DMA. *Polymer Testing*, 30(2), 236–242. https://doi.org/10.1016/j.polymertesting.2010.12.003

Swain, R., Nagamani, R., & Panda, S. (2015). Formulation, in vitro characterization and stability studies of fast dispersing tablets of diclofenac sodium. *Journal of Applied Pharmaceutical Science*, 094–102. https://doi.org/10.7324/japs.2015.50715

Tallury, P., Alimohammadi, N., & Kalachandra, S. (2007). Poly(ethylene-co-vinyl acetate) copolymer matrix for delivery of chlorhexidine and acyclovir drugs for use in the oral environment: Effect of drug combination, copolymer composition and coating on the drug release rate. *Dental Materials*, *23*(4), 404–409. https://doi.org/10.1016/j.dental.2006.02.011

Tang, M., Hou, J., Lei, L., Liu, X., Guo, S., Wang, Z., & Chen, K. (2010). Preparation, characterization and properties of partially hydrolyzed ethylene vinyl acetate copolymer films for Controlled Drug Release. *International Journal of Pharmaceutics*, *400*(1-2), 66–73. https://doi.org/10.1016/j.ijpharm.2010.08.031

Tiboni, M., Campana, R., Frangipani, E., & Casettari, L. (2021). 3D printed clotrimazole intravaginal ring for the treatment of recurrent vaginal candidiasis. *International Journal of Pharmaceutics*, *596*, 120290. https://doi.org/10.1016/j.ijpharm.2021.120290

Vaz, V. M., & Kumar, L. (2021). 3D printing as a promising tool in personalized medicine. *AAPS PharmSciTech*, *22*(1). https://doi.org/10.1208/s12249-020-01905-8

Wang, K., & Deng, Q. (2019). The thermal and mechanical properties of poly(ethylene-co-vinyl acetate) random copolymers (PEVA) and its covalently crosslinked analogues (cpeva). Polymers, 11(6), 1055. https://doi.org/10.3390/polym11061055

Xu, P., Li, J., Meda, A., Osei-Yeboah, F., Peterson, M. L., Repka, M., & Zhan, X. (2020). Development of a quantitative method to evaluate the printability of filaments for fused deposition modeling 3D printing. *International Journal of Pharmaceutics*, *588*, 119760. https://doi.org/10.1016/j.ijpharm.2020.119760